Proceedings of the 9th International Conference on Physical Modelling in Coastal Engineering (Coastlab24)

Delft, Netherlands, May 13-16, 2024

Conference Paper, DOI: 10.59490/coastlab.2024.691

GENERATION OF SCALED LONG-PERIOD SHIP WAVES IN A PUMP-DRIVEN FLUME

CHRISTINA CARSTENSEN[1], FABIAN KARL[1], GREGOR MELLING[1], BERNHARD KONDZIELLA[1], LARS TRETAU[1]

1 Federal Waterways Engineering and Research Institute, Germany, christina.carstensen@baw.de

ABSTRACT

Experimental investigations on the generation of long-period, primary ship waves using a pump-driven technique in a closed-circuit flume are presented. Long-period ship waves can have a major impact on river banks and engineering structures. As larger ship dimensions accompanied by a corresponding rise in loads are expected in the future, the characterisation of long-period ship waves and understanding their impact on bank protection and engineering structures is crucial, especially for appropriate design. Our study combines a closed-loop PID controlled wave generation with a numerical finite difference method (FDM) model. This setup offers the advantage of generating repeatable waves at arbitrary positions along the test section of the laboratory flume. The experiments conducted demonstrate a good reproduction of a scaled long-period ship wave signal (1:10) in a distance of approximately 9 m from the flume inlet. The combination of the PID controlled pump-driven technique with a numerical model provides a solid basis for further studies on ship-induced loads, with the aim to predict future wave loads, better understand the wave-structure-interaction and to mitigate potential damage.

KEYWORDS: Primary Ship Wave, Closed-Circuit Flume, Wave Generation, Laboratory Scale, Finite Difference Method.

1 INTRODUCTION

Ships travelling through confined waterways create a wave field that exert high hydraulic loads on the surrounding banks and engineering structures. The waves are induced as a water volume is displaced by the moving ship and then refilled with a return flow to the stern of the ship. In the bow and stern of the ship increased pressure causes the water level to rise, while alongside the ship low pressure leads to a reduced water level. This system of a positive bow wave, a long trough called drawdown and a positive stern wave is known as the primary wave system (Figure 1). In addition, a secondary wave system develops at the bow and stern of the ship, which consists of short-period, oscillating waves.

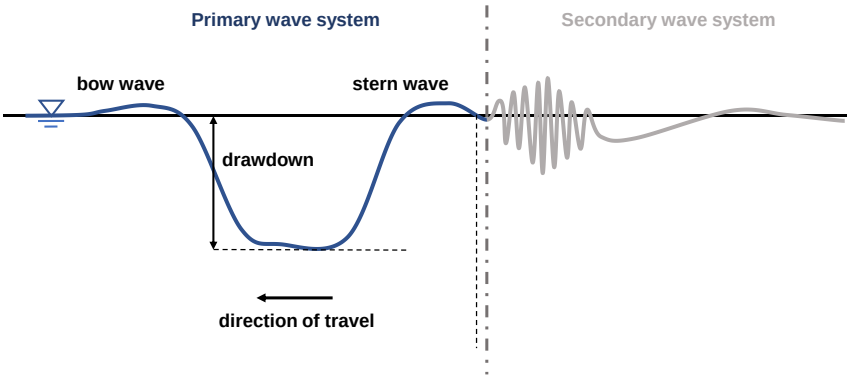

Figure 1: Schematic illustration of the ship-induced wave system (after Carstensen et al., 2023).

The long-period, primary wave system can have a major impact on waterways and their surroundings. In the last 20 years, an increasing number of cases of damage to the engineering structures, groynes and revetments on waterways due to primary ship wave loads have been identified, e.g. in the Elbe estuary (Ohle, N. and Zimmermann, C., 2003; Melling et al., 2020). Furthermore, the size of ships is continually increasing and therefore, even greater damage to banks and structures are expected. However, design approaches for engineering structures and methods for predicting the characteristics of ship-induced long-period, primary waves and their effects, e.g. on the structural stability, are not yet available. It is therefore necessary to analyse ship waves and corresponding loads, especially because higher impacts must be expected in the future.

Experimental methods allow characteristics of primary, long-period ship waves and their effects to be studied in a controlled parameter space. To the best of the authors knowledge, no laboratory experiments on generating long-period ship waves in an experimental flume have been conducted so far. Only within tsunami research long-period wave generation

techniques have been widely tested (e.g. Rossetto et al., 2011; Goseberg et al., 2013). Accordingly, there is no generally accepted method for generating long-period ship waves in a laboratory flume.

In order to investigate the stability of banks and structures under the load of a long-period ship wave in a physical experiment, the first step is to reproduce the relevant parts of the primary wave component in the laboratory. For this purpose, a new pump-driven closed-circuit flume was built, upgraded to enable the generation of the 2D long-period waves and successfully validated (Carstensen et al., 2023). With this setup, the characteristic drawdown and stern wave of the primary ship wave can be modelled and thus the wave dynamics, as a decisive factor in the interaction with banks and structures, can be studied.

The generation method is continuously under development. In this study, we focus (i) on adjusting the control system used for the wave generation to improve the repeatability of the experiments and (ii) on applying a combination of the control system with a numerical finite difference method (FDM) model to facilitate the generation of desired wave forms at any position along the test section. Based on the presented results from the generation of both generic and exemplary primary, long-period ship waves, the performance of the applied method is evaluated with regard to future tasks.

2 PUMP-DRIVEN WAVE GENERATION

2.1 Closed-Circuit Flume

Experiments were performed in the 0.6 m wide closed-circuit flume at the Federal Waterways Engineering and Research Institute (BAW) in Hamburg, Germany. The experimental flume has a rectangular test section of 36 m length, 0.6 m width and 1 m height. At both ends of the test section, an inlet and outlet element of approximately 5 m length is connected to a lower-lying pipe, forming a closed-circuit system. Two parallel impeller pumps are installed inside the pipes, capable of generating flow in both directions. The rotational speed of the pumps is steplessly adjustable, a flow reversal is also possible during the test. The control of the flume is integrated into the laboratory automation system and is operated via a software interface.

For generating long-period waves, an impermeable dividing wall was installed separating the rectangular section into a longer test section of around 35 m and a shorter reservoir section of around 12 m. By using the pumps, water is moved within the flume either from the reservoir section into the test section, or vice versa. Through this, a controlled positive or negative water level change and a propagating wave into the test section are generated. Wave gauges (DHI) at the flume inlet and in a distance of approximately 9 m from the inlet were used to measure the water surface elevation with an accuracy of ±1 mm. A 10 m long sloped beach (1:20) was installed at the end of the test section to dampen reflections at the dividing wall during the wave generation. By this, the waiting time between each test run for ensuring a still water level before the start of each experiment is reduced.

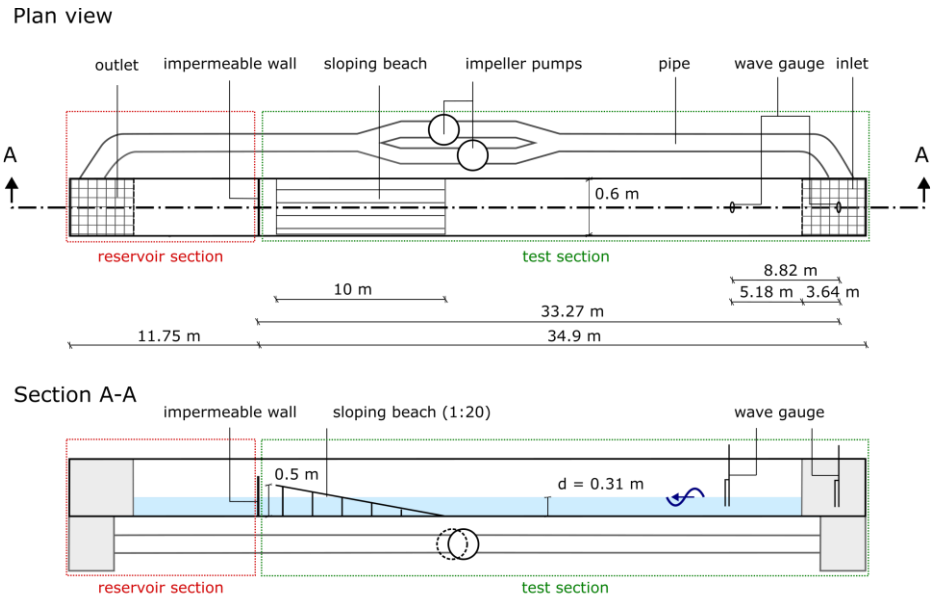

Figure 2: Schematic drawing of the flume, top view and side view.

2.2 Control Setup

A proportional-integral-derivative (PID) controller is used to control the impeller pumps. Applying the PID controller in a closed-loop control system, the measured water level in the flume inlet is continuously compared to a given target water

level of the input wave form. The PID controller minimizes the deviations between the measured and the target water level by adjusting the rotation rate and direction of the pumps in order to adjust the water volume that is pumped into or out of the test section. The closed-loop generation with PID was successfully validated and proved to be suitable for generating different target waves at the inlet of the flume. More details on the applied PID control system and the validation of the setup can be found in Carstensen et al. (2023).

For a tighter control and to improve the repeatability of the generated waves, a combination of a closed-loop and open-loop control can be optionally used. For combining both control methods, the first test run is performed with a closed-loop PID-control, while the repeat measurements are performed with an open-loop control. During the first run the output calculated by the controller to drive the pumps is recorded. For the second run, the recorded controller output is used as the pump-driving target time series in an open-loop control. Results for the combined control for exemplary wave forms are shown in Section 3.1. However, the closed-loop controlled wave generation is generally preferred due to the ability to actively compensate for disturbances (cf. Section 4.1) and was therefore used for further tests in which waves were generated at other positions in the flume (cf. Section 2.3).

2.3 Numerical Model

For the closed-loop control, the instantaneous water level as the process variable for the PID controller is measured as close as possible to the pumps to avoid dead time. Thus, a given target wave form is generated in the inlet to the test section. To generate the target wave form at other positions, a 1D numerical model is used to simulate wave propagation and transformation in the flume, allowing the input signal to be back-calculated. Through this, input signals as setpoints for achieving the target wave form at any position in the test section can be determined.

An FDM model is applied to calculate the input signal for the closed-loop controlled wave generation. The FDM model simulates the wave propagation based on the 1D shallow water equations (cf. Saint-Venant, 1871). Taking into account the flume bathymetry and the friction term derived from the Manning's equation (Manning, 1891), the wave propagation is given by the 1D partial differential Equations (1) and (2):

$$\frac{\partial q}{\partial t} + \frac{\partial (hu^2)}{\partial x} + g \cdot h \cdot \frac{\partial \eta}{\partial x} = - \frac{g n^2 |q| q}{r^{\frac{4}{3}}}, \tag{1}$$

$$\frac{\partial h}{\partial t} + \frac{\partial q}{\partial x} = 0 , \tag{2}$$

where the term $\frac{\partial (hu^2)}{\partial x}$ represents the divergence, $g \cdot h \cdot \frac{\partial \eta}{\partial x}$ the transport and $\frac{g n^2 |q| q}{r^{\frac{4}{3}}}$ the friction, with

$r = \frac{w \cdot h}{w + 2h}$,
$q = h \cdot u$,
t: time (s),
x: distance (m),
q: 1D-discharge (m³/s),
h: water level (m),
u: flow velocity (m/s),
n: Manning's roughness coefficient (-),
g: gravitational force (m/s²),
r: hydraulic radius (m),
η: surface elevation (m),
w: flume width (m).

To implement the FDM model, following difference equations (3) and (4) were derived:

$$q[k,i] = q[k-1,i] - dt \cdot \left(\frac{d\left(\frac{q^2}{h}\right)}{dx} + g \cdot h[i] \cdot \frac{d\eta}{dx} + g \cdot n^2 \cdot q[k,i] \cdot \frac{\sqrt{q[k,i]^2}}{r[i]^{4/3}} \right), \tag{3}$$

$$\eta[k,i] = \eta[k-1,i] - dt \cdot \frac{dq}{dx}, \tag{4}$$

with index of time k and index of distance i.

Since the inflowing discharge q which is required to calculate the central difference quotient $d\left(\frac{q^2}{h}\right)/dx$ at the inlet to the test section is not known, the divergence term is neglected here as a boundary condition. As the water level is given as a boundary condition, $\frac{dq}{dx}$ is not needed to be calculated at this point. The Manning's roughness coefficient n was set to 0.01 based on given values for smooth brass and glass pipes as well as semi-circular smooth metal flumes from King and Brater, 1963. The flume shape is taken into account in the hydraulic radius.

The input signal for generating the target wave form at any position in the test section is calculated by inverting the time components by rearranging the difference equations (3) and (4) to

$$q[k-1,i] = q[k,i] + dt \cdot \left(\frac{d\left(\frac{q^2}{h}\right)}{dx} + g \cdot h[i] \cdot \frac{d\eta}{dx} + g \cdot n^2 \cdot q[k,i] \cdot \frac{\sqrt{q[k,i]^2}}{r[i]^{4/3}} \right), \quad (5)$$

$$\eta[k-1,i] = \eta[k,i] + dt \cdot \frac{dq}{dx}, \quad (6)$$

while the target position is applied as a new source boundary with given target water level of the desired wave form. $d\left(\frac{q^2}{h}\right)/dx$ is again neglected at this position. As boundary conditions of the reverse simulation, the origin of the wave was defined as being at the flume inlet and the wave propagation is directed into the test section, with a still water level before and after the simulation run. Reflections from installations in the test section (e.g. the sloped beach or the dividing wall, cf. Section 2.1) are not taken into account for purposes of simplification.

The FDM model was validated by comparing measured water level signals at different positions along the test section from several test runs with results from the FDM forward simulation. Figure 3 (right) shows the measured water surface elevation compared to the forward simulation result at a distance of 9 m from the inlet to the test section, using the measured water level signal at the inlet as input signal for the FDM simulation run (Figure 3, left). The measured water surface elevation from the laboratory is well reproduced by the FDM model, although at the wave's minimum and maximum values deviations occur, which increase towards the end of the signal due to entering reflections caused by the sloped beach (c.f. Section 4). For the purposes of this study, the FDM model results are deemed sufficiently accurate.

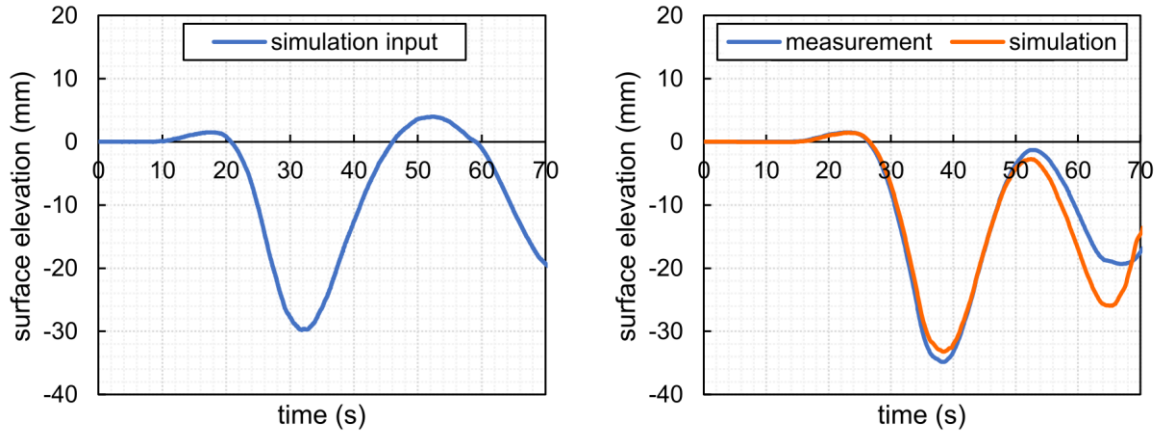

Figure 3: Validation of the FDM model: Measured wave signal at the inlet to the test section as simulation input (left) and measured water surface elevation compared to simulation output at 9 m distance to the inlet (right).

3 GENERATION OF LONG-PERIOD WAVES

3.1 Combination of Closed-Loop and Open-Loop Wave Generation

A combination of a closed-loop PID control with an open-loop control was investigated and compared to experiments generated under closed-loop PID control only (cf. Section 2.2). A solitary wave and a realistic primary ship wave were generated in the flume inlet under the two different control system setups: First, three test runs were conducted using a closed-loop PID control only. Second, the combined control was applied by first generating a closed-loop controlled wave and afterwards using the measured controller output for an open-loop generation of three repeat measurements. For the closed-loop control, the PID control parameters (i) proportional gain factor K_P, (ii) integral time T_I and (iii) derivative time T_D (more details on the PID controller settings are found in Carstensen et al., 2023) were kept almost constant; due to the steep gradients and short periods of the solitary wave, K_P had to be increased to reproduce the target signal. A summary of the hydrodynamic

parameters and the PID control parameter settings is given in Table 1.

Table 1. Wave parameters (laboratory scale) of generated waves for combined closed-loop and open-loop control.

	Water Depth (m)	Wave Period (s)	Wave Height (m)	Drawdown Height (m)	K_P (-)	T_I (s)	T_D (s)
Solitary Wave	0.31	25.6	0.060	-	2	6.5	1.285
Realistic Ship Wave	0.31	33	0.030	0.029	1.7	6.5	1.285

In Figure 4, a solitary wave is shown generated at the flume inlet with a closed-loop control only (left) and under a combined control (right). When comparing the results from both control system setups, a better repeatability was achieved with the combined control than with the closed-loop control only. The recorded wave signals from the combined control show a high agreement between the individual repeat measurements, while minor deviations between the measured signals occur for the closed-loop controlled waves. As for the wave form, small deviations between the target signal and the generated wave signals are found in the backward slope regarding the steepness.

Figure 5 shows a realistic ship wave, whose shape is based on results from experiments carried out with a model ship in a test basin at BAW. The measurements were taken close to the banks of a trapezoidal channel. The original data set of the measured primary wave induced by the model ship was modified by doubling the wave period, while the drawdown height and primary wave height remained the same. As seen in Figure 5, right, a high repeatability is found for the combined control. But also for the closed-loop control only, a good repeatability is seen, tending to be even better. In terms of reproducing the target signal, the drawdown wave was well generated and only the stern wave at the end of the signal was not accurately reproduced; the target stern wave height was exceeded by the generated waves. This deviation is probably caused by a re-entering reflexion from the end of the test section, which is further discussed in Section 4.1.

The results show that the combined control provides an improved or similarly good repeatability. However, as the closed-loop control offers advantages regarding the influence of disturbances, further tests are carried out with closed-loop control only. This is discussed in more detail in Section 4.1.

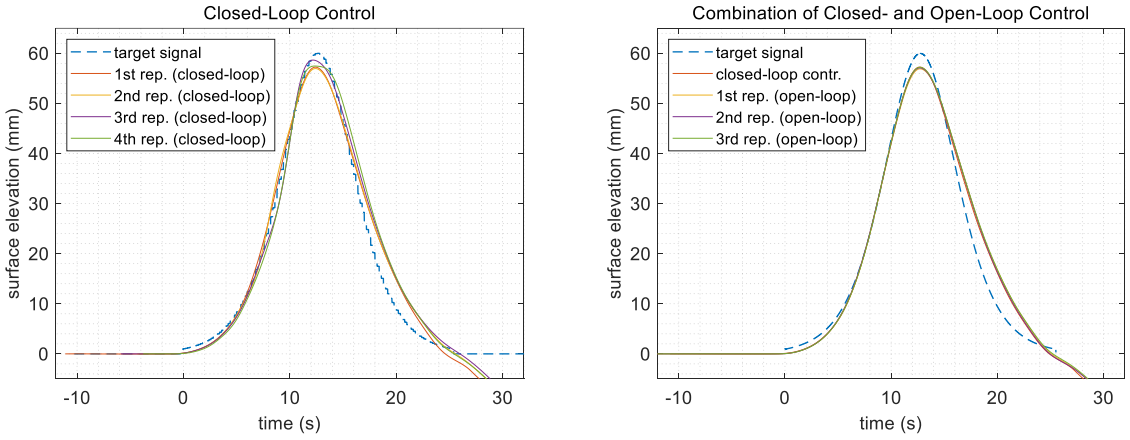

Figure 4. Comparison between closed-loop controlled solitary wave generation (left) and combined closed- and open-loop controlled solitary wave generation.

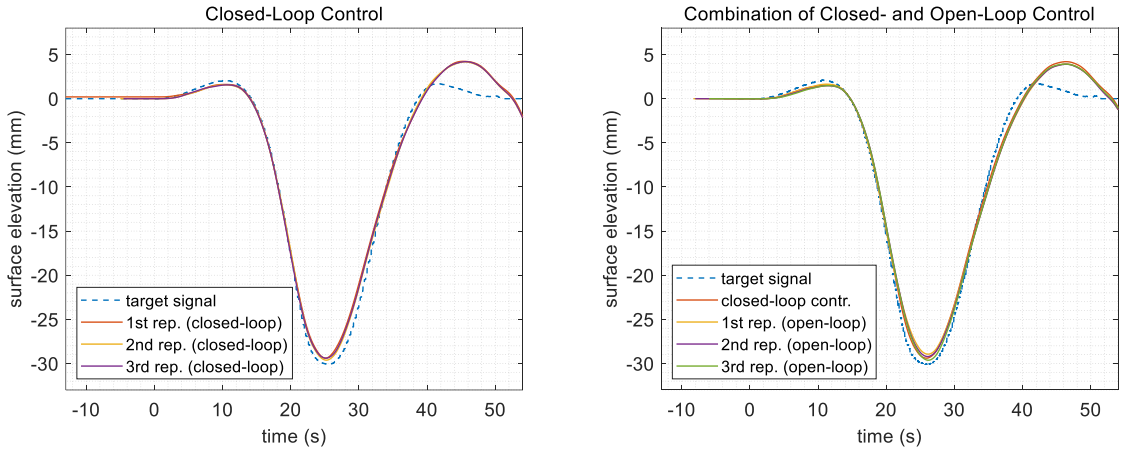

Figure 5: Comparison between closed-loop controlled primary ship wave generation (left) and combined closed- and open-loop controlled primary ship wave generation.

3.2 Closed-Loop Wave Generation in Combination with a Numerical Model

A sinusoidal wave and a realistic primary ship wave were generated at a distance of 5.18 m from the beginning of the test section and approximately 9 m from the flume inlet. The wave generation was performed with a closed-loop PID control only, the input target signal required for the PID control was calculated by the FDM model. Table 2 summarises the hydrodynamic parameters and the applied PID control parameters.

Table 2. Wave parameters and target position (laboratory scale) of generated waves.

	Water Depth (m)	Wave Period (s)	Wave Height (m)	Drawdown Height (m)	Target Wave Position (m)	K_P (-)	T_I (s)	T_D (s)
Sinusoidal Wave	0.31	30	0.08	-	5.18	1.7	6.5	1.285
Realistic Ship Wave	0.31	33	0.03	0.029	5.18	1.7	6.5	1.285

Figure 6 on the left shows the input signal calculated from the FDM model and the corresponding waves generated in the flume inlet, while on the right, the desired sinusoidal wave form is compared to the measured wave signals at the target position. At the target position, especially the second part of the measured wave signals are in good agreement with the desired sinusoidal wave form. Both the descending slope at the beginning and at the end as well as the upward slope in the middle of the wave are well reproduced. Only small deviations are found at the wave peak, where the measured signals are 2-5 mm lower than the target value. However, higher deviations are found at the wave trough, where the measured values exceed the target value by 10-15 mm. Also the first descent of the wave was not entirely reproduced.

Similar deviations were found at the flume inlet, where the calculated input signal was given as setpoint for the PID control (Figure 6, left): The steep descent at the beginning was not generated well and deviations occur especially in the wave trough (2-7 mm). The positive, upward slope and the wave peak align well with the input signal, whereas deviations are found again for the last descent. It can therefore be observed that the deviations found in the inlet propagate along the test section as expected and thus influence the results at the target position. This is discussed in more detail in Section 4.2.

The realistic primary ship wave could be reproduced well at the target position with some exceptions, as seen in Figure 7, right. The bow wave and the descending slope of the drawdown of the measured signals agree well with the desired wave form. Deviations occur at the lowest point of the signal: The generated drawdown signals are lower; the measured minimum values deviate from the target value by approximately 3 mm. However, the beginning of the rising slope of the drawdown is well reproduced, while halfway up, the measured signals again differ from the target signal. The measured stern wave is lower than the target value by approximately 2.5 mm.

For the generation of the calculated input signal in the flume inlet, a good agreement between the input signal and the repeatably generated waves is found (Figure 7, left). Only at the end of the wave at the backward slope of the stern wave, the measured signals deviate from the input signal having their wave peak approximately 5 s later and exceeding the maximum value of the target signal by 2.5 mm (cf. Section 3.1).

Since a good reproduction of the input signal in the inlet has been achieved, the deviations at the target position are attributed to model effects and the accuracy of the FDM model, which is discussed in Section 4.2.

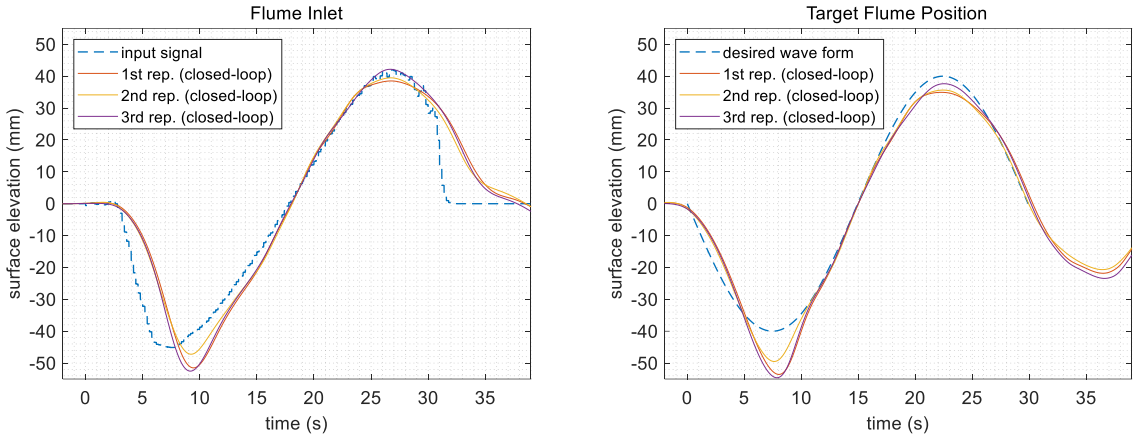

Figure 6: Measured waves at the inlet to the test section in comparison to calculated target signal (left) and measured waves at the target position in comparison to desired sinusoidal wave form (right).

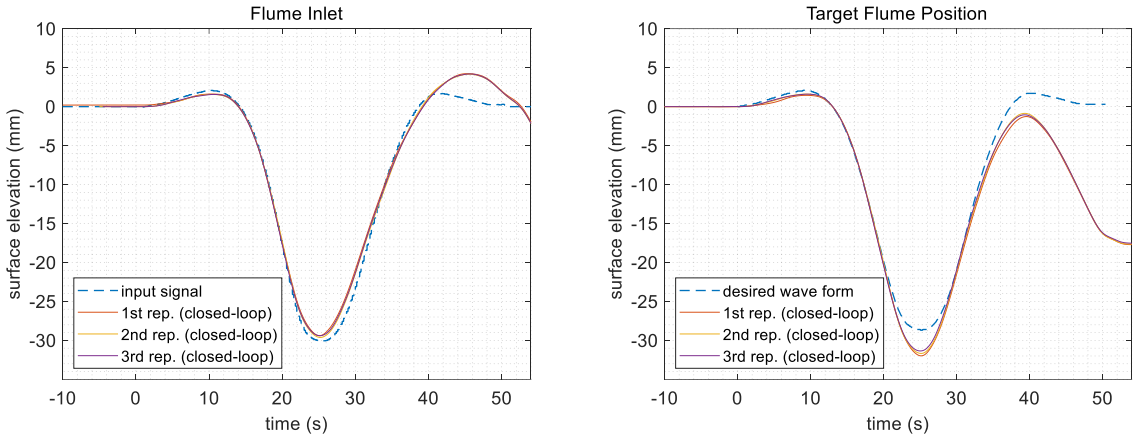

Figure 7: Measured waves at the inlet to the test section in comparison to calculated target signal (left) and measured waves at the target position in comparison to desired primary ship wave form (right).

4 DISCUSSION

4.1 Control Setup

The use of a closed-loop controlled wave generation combined with an open-loop control provided a similarly good repeatability as the closed-loop control only. Nevertheless, the closed-loop PID control is recommended for future experiments and was also used for the wave generation supported by the FDM, as it offers additional advantages: The PID control compensates for disturbances, e.g. small differences in the initial state such as residual unsteadiness from previous tests or slightly different initial water levels (despite careful precautions).

However, results from this study and also from previous studies by Carstensen et al., 2023 using a closed-loop control only, showed that steep gradients are difficult to generate and deviations from the target steepness occur. The reason for this was found in the behaviour of the frequency converter: The pump-driving frequency converter is operated with a ramp, so that the selected frequency (either given by the PID controller or manually defined) is approached at a pre-set, controlled rated ramp. The ramp applies for both accelerating and decelerating, i.e. for generating positive and negative gradients. For the here conducted experiments, the ramp was lowered to a value of 10 s from standstill to full frequency. Thus, the frequency ramp of 10 s limits the accelerating speed of the pumps and therefore the steepness of the gradients to be generated. A further reduction of the ramping time was not practical as the ramp acts as a protection against damage through abrupt operation of the pumps. Gradients that require a faster increase of the pump speed cannot be produced. The observed deviations of the generated solitary waves from the target wave at the backward slope (see Section 3.1, Figure 4) can therefore be attributed to the frequency converter ramp which limits the rate of water level change.

It should be further noted that, at the present state, target signals are also limited in length: Reflections from sloped beach at the end of the test section re-enter the wave gauge after approximately 40 s and are superimposed with the incoming wave, affecting the agreement with the target wave signal. This was observed for the generated realistic ship wave, where deviations

from the target signal were found after approximately 40 s at the stern wave (see Figure 5). A future task is therefore to include expected reflections in the target signals, in case they are exceeding lengths of 40 s, in order to compensate them.

Nevertheless, if the wave generation takes place within these limits regarding the gradient steepness and, as far reflections are not yet included in the target signal, the signal length, the closed-loop PID control provides a good and repeatable reproduction of the desired wave form and is well suited for future long-period wave generation experiments.

4.2 FDM Model Performance

The combination of the pump-driven wave generation technique with a numerical FDM model proved to be suitable to generate desired waves at other positions in the test section. The results showed that the wave transformation is already well compensated by the calculated input signal and the general shape is well met.

For generating the desired wave form at the target position, the calculated input signal to be generated at the flume inlet has to be reproduced as accurately as possible. To achieve this, the input signal must lie within the limits of the pump capability, particularly with regard to the wave steepness (cf. Section 4.1). As shown in Section 3.2 for the generation of the sinusoidal wave, it may occur that even if the desired wave form fulfils the requirements for the wave steepness, the back-calculated input signal might no longer lie within these limits due to the included wave transformation and thus cannot be reproduced satisfactorily. The steep slope of the investigated sinusoidal wave forced the PID controller to rapidly compensate for the control error, which led to an overshoot in the wave trough. If the signal generated in the inlet to the test section differs from the input signal given by the FDM model, as seen in the wave trough in Figure 6 on the right, this will result in a deviation of the generated wave at the target position from the desired wave form on which the FDM calculation was based.

For the realistic ship wave, the wave slopes within the limits could be generated well at the inlet to the test section, so that a mostly good agreement with the desired wave form was also observed at the target position. Here, the remaining deviations occur for two reasons: firstly, the accuracy of the FDM model is not yet high enough, which can be seen particularly at the lowest point of the drawdown; secondly, the influence of the reflections from the end of the test section due to the length of the wave signal are found in the stern wave. As already discussed in Section 4.1, reflections occur according to the measuring position (here after approximately 35 s), superimposed on the recorded signal. At this position, the reflections lead to a lower water level compared to the desired water level.

For future investigations, the two aspects regarding the steepness and the signal length must be taken into account when selecting target wave signals in order to achieve a good reproduction of a desired wave form at a target position in the test section. Future work could already include the reflections occurring in the flume in the calculation. The improvement of the FDM model for better representing the flume and thus for a more accurate modelling of the waves in both forward and backward simulation is ongoing work. Furthermore, the FDM model should also be evaluated in terms of its performance and limitations when generating desired waves at positions with greater distance to the inlet. Nevertheless, the numerical model provides a good addition to the closed-loop PID controlled generation method and contributes to a greater flexibility in terms of a wave generation at other positions in the test section.

5 CONCLUSION

A pump-driven technique for generating long-period waves and particularly primary, long-period ship waves is presented. In this study, the experimental method was successfully complemented by a numerical FDM model that enables waves to be generated at any position along the test section of a closed-circuit flume. A scaled, long-period primary ship wave (1:10) was generated at approximately 5 m distance from the starting point of the test section with only minor deviations from the desired wave form. Furthermore, the feasibility limits of the system were identified and, taking these into account, the closed-loop PID controlled generation was proved to be a suitable technique for performing repeatable experiments.

The presented generation technique enables modelling the dynamics of the primary ship wave, including the drawdown and the transverse stern wave, in a large-scale laboratory setup. Expanding the method with a numerical model to produce waves at various locations in the test section opens up new possibilities for studying the wave interaction with engineering structures or bank vegetation in a physical model. Future work will focus on continuous improvement of the generation method and the numerical model. Additionally, other hydrodynamic parameters such as currents will be measured and analysed to achieve the most accurate reproduction of the natural primary ship wave. This methodology, coupled with the experimental facility, serves as an effective tool for future investigations of long-period ship wave characteristics and for studying bank and structure stability under ship-induced loads.

REFERENCES

Carstensen, C., Melling, G., Kondziella, B., and Tretau, L., 2023. Pump-Driven Generation of Long-Period Ship Waves in Experimental Flumes, *Proceedings of the 40th IAHR World Congress. Rivers Connecting Mountains and Coasts,* Vienna, Austria, pp. 3367–3375. DOI: 10.3850/978-90-833476-1-5_iahr40wc-p1563-cd.

Goseberg, N., Wurpts, A., and Schlurmann, T., 2013. Laboratory-scale generation of tsunami and long waves, *Coastal*

Engineering 79 (1), pp. 57–74. DOI: 10.1016/j.coastaleng.2013.04.006.

King, Horace Williams; Brater, Ernest Frederick, 1963. Handbook of hydraulics for the solution of hydraulic problems, McGraw-Hill, New York.

Manning, R., 1891. On the flow of water in open channels and pipes, *Transactions of the Institution of Civil Engineers of Ireland* (20), pp. 161–207.

Melling, G., Jansch, H., Kondziella, B., Uliczka, K., and Gätje, B., 2020. Evaluation of optimised groyne designs in response to long-period ship wave loads at Juelssand in the Lower Elbe Estuary. 28, *Die Küste* (89). DOI: 10.18171/1.089103.

Ohle, N. and Zimmermann, C., 2003. Untersuchungen zu den Deckwerksverwerfungen am Nordufer der Elbe, *Mitteilungshefte des Ludwig-Franzius-Instituts* (89).

Rossetto, T., Allsop, W., Charvet, I., and Robinson, D.I., 2011. Physical modelling of tsunami using a new pneumatic wave generator, *Coastal Engineering* 58 (6), pp. 517–527. DOI: 10.1016/j.coastaleng.2011.01.012.

Saint-Venant, A.Jean Claude Barré de, 1871. Théorie du mouvement non permanent des eaux, avec application aux crues des rivières et a l'introduction de marées dans leurs lits, *Comptes Rendus de l'Académie des Sciences*.